3*d* metal nanowires and clusters inside carbon nanotubes: Structural, electronic, and magnetic properties

Viktoria V. Ivanovskaya,[1] Christof Köhler,[2] and Gotthard Seifert[1]
[1]*Institute für Physikalische Chemie und Elektrochemie, Technische Universität Dresden, 01062 Dresden, Germany*
[2]*Center for Computational and Material Science, Universität Bremen, 28359 Bremen, Germany*
(Received 1 September 2006; revised manuscript received 9 November 2006; published 9 February 2007)

The structure and the properties of the quasi-one-dimensional composites, i.e., carbon nanotubes filled with nanowires or clusters of 3*d* metals (M=Ti, Fe, and Zn), have been studied in the framework of the density functional-based tight binding method. We show that the accommodation of nanosized metal species inside carbon nanotubes (CNTs) may lead to essential changes of the structural, magnetic, and electronic properties of the CNTs and the metal species. Especially, we examined the effect of interactions between iron and carbon atoms on the electronic and magnetic properties of the Fe_n@CNT composites by comparing with freestanding Fe wires and clusters. Our calculations support the increasing of the magnetic moments for both wires as well as clusters encapsulated in CNTs in comparison with bulk bcc Fe and show a strong dependence of magnetic moments on the thickness of the wires and on the size of clusters.

DOI: 10.1103/PhysRevB.75.075410 PACS number(s): 81.05.Zx

I. INTRODUCTION

Nanotubes (NTs) and monolithic extended nanocrystallites (nanowires, NWs), two main groups of so-called quasi-one-dimensional nanostructures, have been proved to be promising materials for nanoelectronic, nanolithography, photocatalysis, microscopy and other fields of modern nanotechnologies.[1] During the past few years, much progress has been achieved in fabrication of nanocomposites based on NTs and NWs with a set of advanced properties. One of the promising ways to prepare such composites is to fill the tubes with atoms, molecules, clusters, fullerenes, nanowires, etc.[2–5] For instance, carbon nanotubes (CNTs) filled with such metals as Cr,[6] Fe,[7] Co,[8] Ni,[9] Cu,[10] Ge,[11] etc. have been successfully synthesized via various techniques and routes: by catalytic decomposition of precursors, by arc-discharged method, by chemical vapor deposition, by laser vaporization, etc.

In this context, because of their magnetic properties, low dimensionality, and small volume, CNTs filled with magnetic substances should be promising materials for future nanoscale devices. In particular, numerous forms of Fe-filled multiwalled carbon nanotubes (MWCNTs), including iron wires[12–14] and Fe_n clusters[15] embedded inside carbon walls have been obtained and some structural, electronic, and magnetic properties of such Fe_n@CNT composites have been studied.[16–19] For example, magnetic measurements reveal that Fe-filled carbon nanotubes exhibit enhanced coercivities in comparison to those of bulk iron.[20] In addition, carbon nanotubes serve as an excellent oxidation protection for the wires. Possible application for Fe-filled nanotubes as nanomagnets, sensors for magnetic scanning probe microscopy, in data storage, for high density magnetic recording media, as nanoscale spintronic devices, etc. were proposed; see, e.g., Refs. 21 and 22, and references therein. Very recently the first synthesis of Fe-filled single-walled carbon nanotubes via wet chemistry technique was reported.[23]

Theoretically, the composites formed by linear iron atomic chains,[24] as well as by Fe NWs (Refs. 25 and 26) inside CNTs have been examined. It has been shown that the magnetic moments of iron in Fe-filled CNTs are enhanced, compared with bulk Fe. However, while some theoretical studies have been performed for encapsulated iron wires, much less information is known on the structural and electronic properties of related M_n@CNT composites, where M_n are wires of other transition metals inside carbon nanotubes.[27,28] Moreover, no data are available about the electronic and magnetic properties of the other mentioned class of composites—metal clusters inside CNTs.

In this study, we present the results of a systematic theoretical investigation of the structural, electronic, and magnetic properties of several groups of M_n@CNT composites to learn more about the nature of these materials. First, we performed *within the same method* a comparative study of the structural and electronic properties of single-walled carbon nanotubes filled with 3*d* metallic nanowires or clusters (M=Ti, Fe, and Zn). These metals were chosen for the following reasons. The interactions of metal atoms placed inside CNTs with the tube walls are important for understanding the properties of the M_n@CNT composites. For this purpose, Ti-C, Fe-C, and Zn-C systems are contrasting examples of the metal-carbon interaction and present prospects for a comparison of the electronic properties and chemical bonding depending on their possible nanocomposite forms. Indeed, for the Ti-C system ($Ti3d^24s^2$), the highly stable TiC_x phase is known, which belongs to the family of *d*-metal carbides with strong covalent bonding and it exhibits extreme hardness, extraordinarily high melting points, and chemical inertness.[29] On the contrary, crystalline iron carbides ($Fe3d^64s^2$) are thermodynamically unstable, whereas zinc ($Zn3d^{10}4s^2$) is known to be practically inert to carbon. To the best of our knowledge no experiments have been reported about the synthesis of Zn_n@CNT or Ti_n@CNT composites, but there are data available on encapsulated single Ti nanocrystals and TiC particles in carbon nanocages.[30,31] Finally, we investigate in more detail through local spin-density functional calculations iron wires and clusters inside CNTs. We studied the effect of encapsulated iron wires in

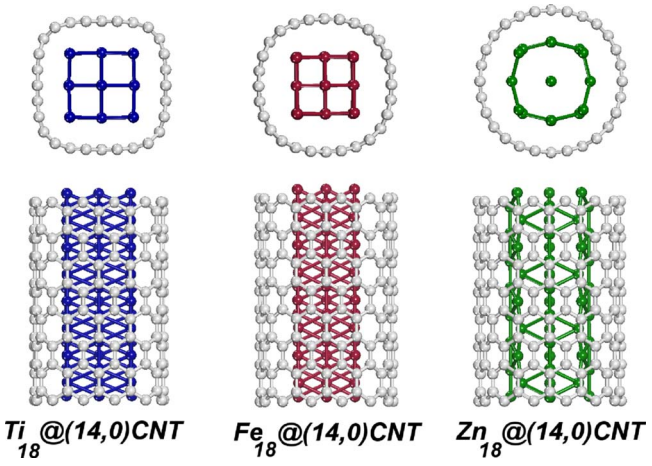

FIG. 1. (Color online) Optimized structures for metal (Ti, Fe, Zn) nanowires encapsulated inside zigzag (14,0) CNT. Views down the axis of the nanotubes and side views are displayed.

comparison with several types of Fe_n clusters inside CNTs on the structural, electronic, and most interesting, magnetic properties of Fe_n@CNT composites.

II. MODELS AND COMPUTATIONAL DETAILS

For the comparative study of the M_n@CNT composites (M=Ti, Fe and Zn) we have used structures with the same number of atoms and starting geometries. Two types of nonchiral carbon NTs, having different electronic properties have been used: metallic armchair (8,8) and semiconducting zigzag (14,0) NTs, with similar diameters of 10.86 and 10.97 Å, respectively. Experiments suggest the appearance of both bcc (α) and fcc (γ) Fe phases in Fe_n@CNT composites.[12–14] Since the iron bcc structure is the most stable phase, in our atomic models the nanowire axis corresponds to the [001] axis in bcc Fe bulk. The same bcc-like wires were studied for Ti_n@CNT and Zn_n@CNT composites, see Fig. 1.

Carbon nanotubes and metallic wires have different periodicity along the z axis. This incommensurability could induce a structural "frustration" on the carbon nanotube and the internal nanowire in M_n@CNTs. The periodicity of bulk bcc titanium is a=3.320 Å, bcc iron is a=2.867 Å. Zinc does not have a stable bcc bulk, but for the comparative analysis we adopted the same atomic ordering for initial structure such as in titanium- and iron-encapsulated wires. For armchair tubes, the periodicity along the axis is 2.46 Å and for zigzag tubes it is 4.26 Å. That means that depending on the type of the M_n@CNT structure we get a minimum mismatch, considering one period of the wire per one armchair and two periods of the wire per one zigzag tube's periods, respectively. The distances between the thickest nanowires and tube walls are close to that, known for bulk metal carbides: TiC ($R_{\text{Ti-C}}$=2.167 Å) and Fe_3C ($R_{\text{Fe-C}}$=1.961÷1.939 Å).[29,32]

In atomic simulations of M_n@CNT composites with metal clusters, two variants of ordering M_n clusters inside the tubes were studied: (i) the M_n clusters are separated from each other, and (ii) the M_n clusters are in close vicinity to each other.

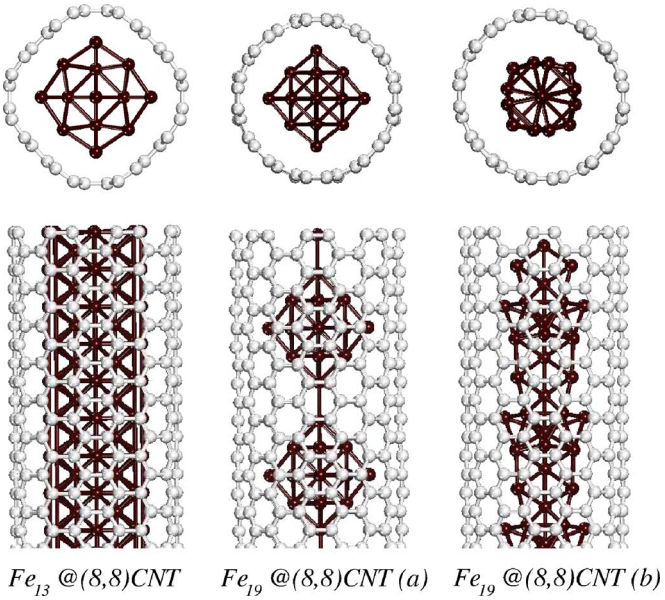

FIG. 2. (Color online) Optimized structures for Fe nanowire and clusters encapsulated inside of armchair (8,8) CNT; (a) clusters are distant from each other for ~2.7 Å; (b) clusters situated close to each other inside of the tube, forming a pseudowire. Views down the axis of the nanotubes and side views are displayed.

The structures of inserted clusters, as in the case of wires, are derived from the atomic ordering of bcc bulk structures, Fig. 2.

In summary, we considered three different morphological types of encapsulated metal wires: M_5, M_9, and M_{13} inside armchair (equivalent to M_{10}, M_{18}, and M_{26} inside zigzag) carbon tubes and three different morphological types of encapsulated clusters: M_6, M_{15}, and M_{19}, for the last two different ordering positions we examined. Hereafter, for the classification of the M_n@CNT composites, we will denote n the number of metal atoms in the unit cell and the configuration of the carbon tube and metal wire. For example, the unit cell of the composite system shown in Fig. 1 consists of 18 Fe atoms inserted in an armchair (14,0) nanotube; this system will further be called as Fe_{18}@(14,0)CNT.

We performed structural optimizations and band structure calculations within density functional theory in its tight-binding approximation (DFTB)[33,34] including spin polarization.[35] The DFTB method is an approximation to fully self-consistent density functional theory. The method has been found to describe the structure and energy of metal-nonmetal nanostructures in a good agreement with experiments and higher-level theoretical methods.[36–38] In our calculations, the DFTB parameters have been extensively benchmarked to DFT LSDA calculations done for similar reference systems. All the composites are described within the supercell approach. Periodic boundary conditions with a set of 10 k points along the tube direction were applied for geometry optimizations, as it has been proved to be sufficient for an appropriate sampling of the Brillouin zone; a larger set of 40 k points was employed for band structure calculations.

No cutoff radii for the range of the Hamiltonian and overlap matrix elements were used. The Ewald technique was used to treat the Coulomb part. The Kohn-Sham orbitals are expressed as a linear combination of Slater type orbitals (LCSTO, 12 per basis function) in a minimal basis representation, i.e., considering the 2*s*, 2*p* carbon valence orbitals and the 3*d*, 4*s*, and 4*p* iron valence orbitals. Such basis is consistent with the DFTB approximations.

III. RESULTS AND DISCUSSION

A. Structure and stability

First, for all M_n@CNTs systems with encapsulated wires, we optimized the lattice parameters along the *z* axis and found that the cell parameters of the tubes are stretched, while those of the metal cores are compressed. The optimized cell parameters of the M_n@CNTs in comparison with the "empty" carbon tubes increase, depending on the filling ratio, of about 3–8 % for the Ti_n@CNT, 1–5 % for the Fe_n@CNT and 1–3 % for the Zn_n@CNT composites. The ratio of the increase depends from the morphology of the wires and reaches its maximum in the case of encapsulation of thick wires.

The optimized structures for some M_n@CNTs composites are shown in Fig. 1, and demonstrate an essential dependence of their morphology from the type of the metal core. For the Ti_{18}@(14,0)CNT, the CNT cross section changes from circular to quadraticlike, due to the strong covalent interactions between "external" atoms of the Ti NW and the carbon atoms of the CNT. These interactions affect even more strongly the shape of the composite with the biggest encapsulated nanowire [Ti_{26}@(14,0)CNT]. Oppositely, for the Fe_{18}@(14,0)CNT, the initial shapes [quadratic-prismatic of Fe wire and cylindrical (14,0) CNT] are preserved without any visible changes after optimization. That indicates the small interatomic Fe-C bonding. The strength of the Fe-C bonding increases when the distances between wire and CNT is decreased; the composites with encapsulated thick Fe_{13}, Fe_{26} wires show a tendency to the formation of quadraticlike cross-section shapes. Experimentally, in most cases, the encapsulation of iron wires inside multiwalled carbon nanotubes was observed. These are more rigid systems than single-walled CNTs and the effects on curvature of the walls after the wire encapsulation will be less pronounced.

For the Zn_{18}@(14,0)CNT, we obtain a reverse situation compared to the Ti_{18}@(14,0)CNT, Fig. 1. After optimization the tube walls remain practically unchanged, whereas the atomic structure of the Zn NW differs substantially. Thus, the starting shape of the bcc-like Zn_{18} wire is unstable and the resulting structure of the wire inside the tube is strongly affected by repulsive interactions between Zn atoms and carbon atoms of the tube wall. The structures of composites with thick Zn_{13}, Zn_{26} wires (having minimal distances between wires and carbon tubes) are unstable and break apart. Only small Zn_5, Zn_{10} wires inside Zn_n@CNT composites are stable and keep their structure without severe changes. The interatomic distances reflect the described perturbation of the systems. In most cases the C-C bond distances are increased and the M–M bond distances are reduced, compared with the corresponding free nanotubes or metal bulk systems, Table I.

TABLE I. Average interatomic distances (Å) for the composites M_{18} inside of zigzag (14,0) CNT.

Bond length, Å/System	C-C	C-M	M–M
Ti_{18}@CNT	1.45	2.51	2.62
Fe_{18}@CNT	1.46	2.63	2.51
Zn_{18}@CNT	1.48	2.64	2.55

In the case of encapsulated clusters, we considered M_n clusters of different size inserted at different distances between each other inside the carbon nanotubes, Table II. The cell parameters of tubes filled with metal clusters remain practically unchanged even for high density of filling (changes do not exceed ~0.5%). The optimization does not affect strongly the composites with small encapsulated titanium and iron clusters (M_6) or clusters far distant from each other. We have found a strong transformation of the structures for large (M_{15},M_{19}) clusters in M_n@CNT, if the clusters were initially located in the vicinity of each other. The resulting composite structure contains "pseudowires" instead of chains of clusters. As an example in Fig. 2 the optimized structures of metal clusters encapsulated inside carbon nanotubes are given for the Fe_n@CNT system. For Zn_n@CNT composites we observe the strongest deviation from the initial structures, the formation of pseudowires is especially unfavorable. That could be explained by the initially unstable shape of Zn clusters (only the smallest free Zn clusters keep the initial geometry after optimization) and by repulsive interactions between Zn atoms and carbon atoms of tube walls.

The incommensurability between the lattice constants of the CNT and the metal wires leads to the above-mentioned stretching of the CNTs and the corresponding compression of the metal wires. The "commensurability problem" does not exist for the composites with encapsulated clusters. Therefore, the C-C bond lengths of systems are closer to those of pure carbon tubes and the M–M bonds are less compressed compared to the systems with encapsulated metal wires. The values of averaged first-neighbor interatomic distances for

TABLE II. Average interatomic distances (Å) for metal wires and clusters inside of armchair (8,8) CNT.

Bond length, Å/system	C-C	C-M	M–M
Fe_{13} wires	1.49	2.57	2.49
Fe_{19} cluster[a]	1.43	2.65	2.61
Fe_{19} cluster[b]	1.43	2.62	2.51
Ti_{13} wires	1.51	2.52	2.66
Ti_{19} cluster[a]	1.43	2.72	2.81
Ti_{19} cluster[b]	1.43	2.63	2.68

[a]Clusters are situated close to each other inside the tube, forming a pseudowire.

[b]Clusters are distant from each other. For Ti_{19} the optimized intercluster distances are ~2.3 Å, for Fe_{19}~2.7 Å.

TABLE III. The formation energy E_{form}, eV/n for Ti, Fe wires and clusters encapsulated in armchair (8,8) CNT, where n is the number of metal atoms in the unit cell.

System	Encapsulated Ti Wires		
	Ti_5@(8,8)CNT	Ti_9@(8,8)CNT	Ti_{13}@(8,8)CNT
E_{form}	0.40	0.50	0.03
System	Encapsulated Ti Clusters		
	Ti_6@(8,8)CNT	Ti_{15}(8,8)CNT	Ti_{19}(8,8)CNT
E_{form}	−0.18	0.10[a]/−0.10[b]	−0.17[a]/−0.48[b]
System	Encapsulated Fe Wires		
	Fe_5@(8,8)CNT	Fe_9@(8,8)CNT	Fe_{13}@(8,8)CNT
E_{form}	−0.21	−0.36	0.30
System	Encapsulated Fe Clusters		
	Fe_6@(8,8)CNT	Fe_{15}@(8,8)CNT	Fe_{19}@(8,8)CNT
E_{form}	−0.09	−0.46[a]/−0.29[b]	−0.66[a]/−0.31[b]

[a]The clusters are situated close to each other with formation of pseudowire inside the tube.
[b]The clusters are distant from each other inside the tube.

some of the optimized M_n@CNT composites with M_n clusters inside the CNT are given in Table II.

To study the stability of M_n@CNTs, we estimated formation energies of the systems as

$$E_{\text{form}} = [E_{\text{tot}}(M_n \text{ @ CNT}) - \{E_{\text{tot}}(\text{CNT}) + E_{\text{tot}}(M_n)\}]/n, \quad (1)$$

where $E_{\text{tot}}(M_n\text{@CNT})$, $E_{\text{tot}}(\text{CNT})$, $E_{\text{tot}}(M_n)$ are the total energies of the M_n@CNT composite, carbon nanotube, and free metal wire or cluster, respectively, and n is the number of metal M atoms per unit cell. The calculated formation energies (E_{form}) for the composites M_n@CNT with encapsulated metal wires and clusters are given in Table III. We consider only the formation energies for the armchair (8,8) CNT, since in this case we have less structural mismatch at the encapsulation, compared to the systems with the zigzag (14,0) nanotube.

In spite of the high carbide-forming ability of titanium, the formation energies for encapsulated Ti wires inside CNTs are slightly positive. This fact could be attributed to the considerable elongation (up to ~8%) of the carbon tube in the composite. However, with the increase of the thickness of the wire, the formation energy is decreased, due to an energy gain by the formation of stronger covalent titanium-carbon interactions; see Table III. For titanium clusters inside CNTs, in contrast to the encapsulated wires, we get negative values for the formation energies. This can be attributed to the almost undisturbed structure of the CNT inside the composite with clusters contrasting to the CNT with encapsulated Ti wires. The calculated formation energies decrease with the size of the clusters, which is connected with a stronger covalent titanium-carbon bonding. The calculations show a preferential ordering of Ti_n clusters distant from each other inside CNT, rather than situated close to each other with the formation of pseudowires, Table III. Hence, according to our calculations for Ti_n@CNT systems, the encapsulation of distant big-sized clusters is preferred.

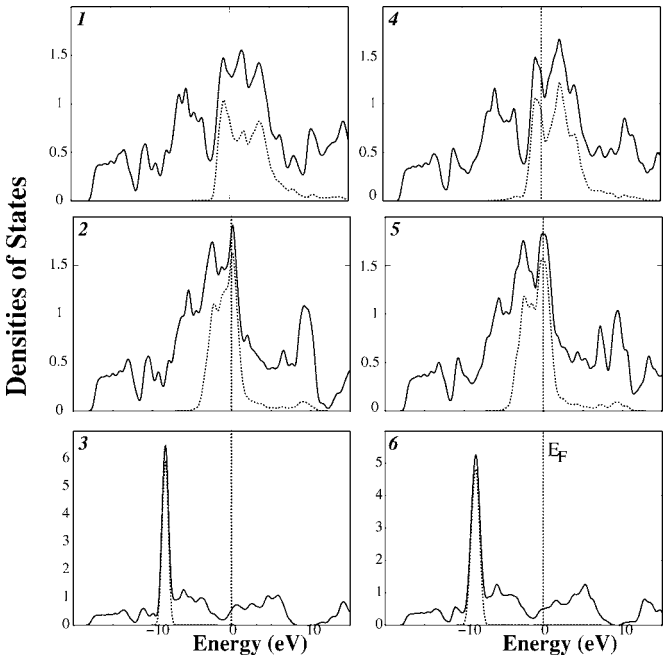

FIG. 3. Total (solid lines) and M3d (dotted lines) densities of states for composites M_9@(8,8)CNT (1–3) and M_{18}@(14,0)CNT (4–6). M=Ti (1,4), Fe (2,5), Zn (3,6). The energy is given (in eV) relative to E_F.

For the Fe_n@CNT systems E_{form} is negative if the carbon tube is not substantially distorted, i.e., the elongation of CNT is less then ~2% and the circular cross section of the tube is not much disturbed. This means that the process of formation of these composites should be exothermic. For thick Fe wires and correspondingly more elongated tubes (up to 5%) the formation energies are positive, see Table III. For Fe_n@CNT composites with participation of wires, the most stable structure results from encapsulation of the medium sized Fe_9 wires; see Table III. Such behavior can be explained, considering the competition between the iron-carbon interaction, which increases with the diameter of the Fe wire, and the structural frustration of the system, which increases with the filling ratio. We have found negative values for the formation energies for CNTs with encapsulated iron clusters. The Fe pseudowires are clearly more stable than the isolated Fe cluster in the CNT, Table III. As far as the cluster fits into the CNT, the formation energy becomes more negative with increasing the cluster size.

Encapsulation of metal clusters or wires inside carbon nanotubes lead to an energetic competition between formation of covalent bonding between metal and carbon atoms and structural frustration induced by cell mismatch. The results suggest that, in general, up to a certain limit, the encapsulation of iron wires is more energetically favorable than encapsulation of clusters of similar sizes. When the diameters of wires reach their critical size and the distortion of the carbon nanotubes becomes significant, the formation energies favor the clustering inside the CNTs, Table III. In this

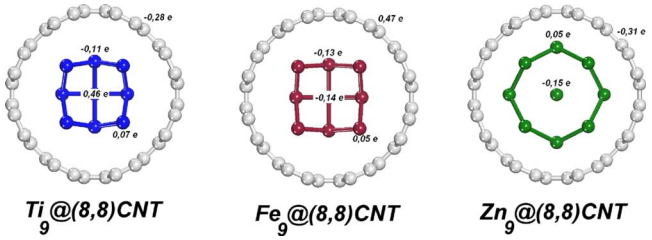

FIG. 4. (Color online) Calculated charges on atoms (e) for medium-sized metal wires inside of armchair (8,8)CNT. Carbon atoms are gray.

case, as we already mentioned, more stable configurations will be closely situated clusters that form pseudowires; however, the formation of distant clusters is also possible. Experimentally, the formations of wires as well as iron nanoparticles are reported,[12–19] but there are no data available about the ratio of synthesis products. We could suppose that the process of formation of encapsulated wires or clusters are competitive, and the result of the synthesis will depend on the particular thermodynamic experimental conditions (carbon-iron ratio, temperature, pressure, presence of catalyst, etc).

Due to instability of free zinc wires, derived from bulk bcc structure, we did not perform energetic estimations for Zn_n@CNT composites. The most structurally stable Zn_n@CNT composites are formed by inserting thin metal wires or small clusters into the CNTs.

B. Electronic and magnetic properties

We discuss now the electronic properties of M_n@CNT composites. The densities of states (DOSs) for M_9@(8,8) and M_{18}@(14,0)CNTs systems are given as examples in Fig. 3. For all considered types of metal wires inside of semiconducting and metallic CNTs, the M_n@CNT composites have a metalliclike behavior. The most essential changes in the electronic structure, when going from Ti_n@CNT to Zn_n@CNT composites, can be interpreted in terms of the metal 3*d* band filling. For Ti_n@CNT structures, the partially occupied Ti3*d* states are placed in the vicinity of the Fermi level (E_F) and are considerably hybridized with the C2*p* states. For Fe_n@CNT composites, the bands in the energy region between −4 and +2 eV consist predominantly of Fe3*d* states. Thus, as well as for crystalline Fe_3C,[39] for these composites the iron 3*d* states are dominant around the Fermi level. Nevertheless, some contribution of the covalent bonds between iron and carbon atoms due to the overlapping of Fe3*d*-C2*p* states can be seen in the energy interval between −5 and −3 eV below the Fermi level. Oppositely, for Zn_n@CNT, the fully occupied Zn3*d* states form a narrow atomiclike DOS peak located far below E_F. Consequently, carbon and zinc valence states are well separated and their hybridization is very weak. Thus, for metalliclike M_n@CNT

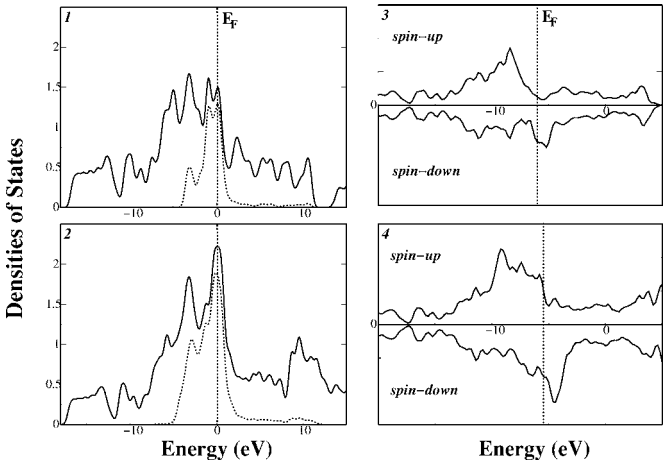

FIG. 5. Total (solid lines) and Fe3*d* (dotted lines) densities of states for composites M_5@(8,8)CNT (1,3) and M_{13}@(8,8)CNT (2,4): non-spin-polarized (1,2) and spin-polarized (3,4) calculations. The energy is given (in eV) relative to E_F.

TABLE IV. The magnetic moments (μ_B/atom) for the Fe wires and clusters encapsulated in armchair (8,8) and zigzag (14,0) CNT. The data for freestanding wires and cluster as well as for bulk iron are given for comparison.

Structure	Magnetic moment, μ_B/atom	Structure	Magnetic moment, μ_B/atom	Structure	Magnetic moment, μ_B/atom
		Wires			
Fe_5@(8,8)CNT	2.80	Fe_{10}@(14,0)CNT	2.80	Fe_5 wire	3.00
Fe_9@(8,8)CNT	2.67	Fe_{18}@(14,0)CNT	2.67	Fe_9 wire	2.78
Fe_{13}@(8,8)CNT	2.62	Fe_{26}@(14,0)CNT	2.62	Fe_{13} wire	2.69
		Clusters			
Fe_6@(8,8)CNT	3.33[b]	Fe_6@(14,0)CNT	3.33[b]	Fe_6 cluster	3.33
Fe_{15}@(8,8)CNT	2.53[a]–2.80[b]	Fe_{15}@(14,0)CNT	2.67[a]–2.80[b]	Fe_{15} cluster	2.93
Fe_{19}@(8,8)CNT	2.63[a]–2.74[b]	Fe_{19}@(14,0)CNT	2.74[c]	Fe_{19} cluster	2.84

[a]The clusters are situated close to each other with formation of pseudowire inside the tube.
[b]The clusters are distant from each other inside the tube.
[c]The structure with close situated clusters inside the tube is changed during the optimization with the formation of an amorphous-like encapsulated iron structure.

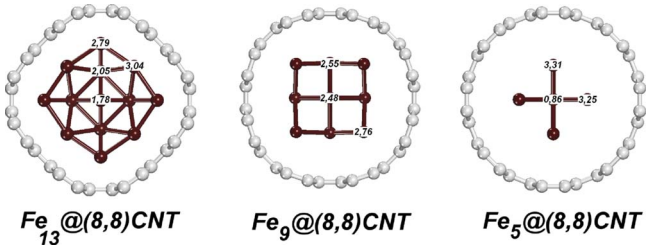

FIG. 6. (Color online) Magnetic moments on atoms (μ_B/atom) for metal Fe wires inside of armchair (8,8)CNT. Iron atoms are black; carbon atoms are gray.

composites the bands near the Fermi energy are of quite different types: for Ti_n@CNT, these bands are of "mixed" nature, i.e., are composed from the Ti3*d*-C2*p* states, whereas for Fe_n@CNT they are mainly of Fe3*d* type, and for Zn_n@CNT they have predominantly carbon 2*p* character. Note that DOSs for M_n clusters inside of both types of carbon nanotubes are also metalliclike, and in general tendencies resemble those of the encapsulated wires.

In Fig. 4 the charge distribution of medium sized M_9 wires inside the armchair (8,8) CNT—as an example—is shown. As one can see, for Fe_9@CNT there is a charge transfer q of 0.47 e^- per unit cell from carbon atoms to iron atoms. The transferred charge is not homogeneously distributed over the iron atoms (see Fig. 4). For Ti_9@CNT as well as Zn_9@CNT systems, we obtain an opposite direction of charge transfer: from metal atoms to carbon; q of the carbon tube per unit cell in Ti_9@CNT ~ -0.28 e, q of the carbon tube in Zn_9@CNT $\sim -0.31e$. For the case of encapsulated metal clusters, the charge transfer strongly depends upon the distances between the clusters inside the nanotubes; for instance, for well-separated Fe_{15} clusters (minimal distance between the clusters $\sim$4.8 Å) inside armchair (8,8) CNT q on iron atoms is equal to ~ -0.44 e^- per unit cell, while when the same clusters are situated close to each other with formation of pseudowire (minimal distance between the clusters $\sim$2.2 Å) $q_{Fe} \sim -0.58$ e^- per unit cell. There is also a certain charge difference for metal atoms of wires and clusters inside the composites, depending on the coordination numbers. The obtained tendencies for the directions of charge transfer, found for encapsulated metal wires, are also preserved for the clusters and are in accordance with that known for iron and titanium carbides.[40]

The magnetic characterization of Fe_n@CNT composites is of special interest for their potential applications.[21,22] We have analyzed the magnetic properties of Fe_n@CNT systems within the DFTB method including spin-polarization.[35] DOS's for spin-up and spin-down states of some Fe_n@CNT composites are given in Fig. 5. The magnetic moments (MM) at the Fe atoms are given in Table IV. No magnetization has been found on the carbon atoms. In accordance with the previous theoretical calculations of encapsulated Fe wires,[25,26] we found a significant enhancement of magnetic moments as for "freestanding" iron wires as well as for encapsulated ones compared to bulk bcc Fe.[41] The reason for such enhancement of MMs is due to the reduced coordination numbers of metal atoms in these systems. As an example, we show in Fig. 6 the distribution of the magnetic moments over the atoms of the wires encapsulated in armchair (8,8) CNT. One can see that highest magnetic moments get the atoms on the border of the wires, i.e., having the lowest coordination numbers. Thin wires, which are well separated from tube walls, present the highest values of MM compared to that of freestanding systems. The calculated magnetic moments for the encapsulated clusters are given in the Table IV. Due to reduced coordination number, MMs for clusters are generally higher then for freestanding wires; see also Ref. 42. After the encapsulation in carbon tubes, the MM of clusters is decreased. Magnetic moments for the clusters forming a pseudowire are similar to MMs of "regular" encapsulated wires and are $\sim 0.1 \div 0.3 \mu_B$/atom lower, compared with those for separated clusters in nanotubes.

IV. CONCLUSIONS

In summary, the atomic models of the quasi-one-dimensional composites—carbon nanotubes filled with nanowires or ensembles of clusters of some 3*d* metals (M=Ti, Fe, and Zn)—have been proposed and their properties analyzed by means of the density functional-based tight-binding method including spin polarization. We showed that the accommodation of metal nanosized structures inside CNTs may lead to essential changes of the structural, magnetic, and electronic properties of these systems. For Ti_n@CNT and Zn_n@CNT composites, considerable structural reconstructions were obtained; for the Ti_n@CNT system, more preferable is the encapsulation of big distant clusters, whereas for Zn_n@CNT composites, the insertion of thin metal wires and small clusters is preferred. For Fe_n@CNT systems, we showed that more favorable will be encapsulation of medium-sized iron wires and clusters in vicinity of each others (with the formation of pseudowire).

We especially examined in more detail the effect of interactions between iron and carbon atoms on the magnetic properties of the iron wires and Fe_n clusters inside CNTs by comparison with freestanding wires and clusters. For Fe_n@CNT systems, an enhanced magnetization in comparison to bulk Fe was found. For all M_n@CNT composites, the metalliclike behavior has been established.

ACKNOWLEDGMENTS

Financial support by the DFG is gratefully acknowledged. V.V.I. thanks RFBR (Grant No. 05-03-32021) and President Grant No. MK-5971.2006.3 for financial support and A. Zobelli for valuable suggestions.

[1] *Carbon Nanotubes: Synthesis, Structure, Properties, and Applications*, edited by M. S. Dresselhaus, G. Dresselhaus, and P. Avouris (Springer, Berlin, 2001).
[2] A. Hirsch and O. Vostrowsky, Top. Curr. Chem. **245**, 193 (2005).
[3] M. Burghard, Surf. Sci. Rep. **58**, 1 (2005).
[4] H. Terrones, F. Lopez-Urias, E. Munoz-Sandoval, J. A. Rodriguez-Manzo, A. Zamudio, A. L. Elias, and M. Terrones, Solid State Sci. **8**, 303 (2006).
[5] V. V. Ivanovskaya, Yu. N. Makurin, and A. L. Ivanovskii, in *Nanostructures: Novel Architectures*, edited by M. Diudea (Nova Science Publishers, New York, 2005), chap. 2.
[6] C. Cuerretpiecourt, Y. Lebouar, A. Loiseau, and H. Pascard, Nature **372**, 761 (1994).
[7] N. Grobert, W. K. Hsu, Y. Q. Zhu, J. P. Hare, H. W. Kroto, D. R. M. Walton, M. Terrones, H. Terrones, Ph. Redlich, M. Rühle, R. Escudero, and F. Morales, Appl. Phys. Lett. **75**, 3363 (1999).
[8] A. Leonhardt, A. Ritschel, R. Kozhuharova, A. Graff, T. Mühl, R. Huhle, I. Mönch, D. Elefant, and C. M. Schneider, Diamond Relat. Mater. **12**, 790 (2003).
[9] N. Grobert, M. Terrones, A. J. Osborne, H. Terrones, W. K. Hsu, S. Trasobares, Y. Q. Zhu, J. P. Hare, H. W. Kroto, and D. R. M. Walton, Appl. Phys. A: Mater. Sci. Process. **67**, 595 (1998).
[10] A. A. Setlur, J. M. Lauerhaas, J. Y. Dai, and R. P. H. Chang, Appl. Phys. Lett. **69**, 345 (1996).
[11] A. Loiseau and H. Pascard, Chem. Phys. Lett. **256**, 246 (1996).
[12] Z. J. Liu, R. C. Che, Z. D. Xu, and L. M. Peng, Synth. Met. **128**, 191 (2002).
[13] A. Leonhardt, A. Ritschel, R. Kozhuharova, A. Graff, T. Mühl, R. Huhle, I. Mönch, D. Elefant, and C. M. Schneider, Diamond Relat. Mater. **12**, 790 (2003).
[14] R. Kozhuharova, M. Ritschel, D. Elefant, A. Graff, A. Leonhardt, I. Mönch, T. Mühl, and C. M. Schneider, J. Mater. Sci.: Mater. Electron. **14**, 789 (2003).
[15] H. Kim and W. Sigmund, J. Cryst. Growth **276**, 594 (2005).
[16] C. Prados, P. Crespo, J. M. González, A. Hernando, J. F. Marco, R. Gancedo, N. Grobert, M. Terrones, R. M. Walton, and H. W. Kroto, IEEE Trans. Magn. **37**, 2117 (2001).
[17] S. Karmakar, S. M. Sharma, P. V. Teredesai, and A. K. Sood, Phys. Rev. B **69**, 165414 (2004).
[18] T. Ruskov, S. Asenov, I. Spirov, C. Garcia, I. Mönch, A. Graff, R. Kozhuharova, A. Leonhardt, T. Mühl, M. Ritschel, C. M. Schneider, and S. Groudeva-Zotova, J. Appl. Phys. **96**, 7514 (2004).
[19] T. Mühl, D. Elefant, A. Graff, R. Kozhuharova, A. Leonhardt, I. Mönch, M. Ritschel, P. Simon, S. Groudeva-Zotova, and C. M. Schneider, J. Appl. Phys. **93**, 7894 (2003).
[20] B. C. Satishkumar, A. Govindaraj, P. V. Vanitha, A. K. Raychaudhuric, and C. N. R. Rao, Chem. Phys. Lett. **362**, 301 (2002).
[21] A. Leonhardt, S. Hampel, C. Müller, I. Mönch, R. Koseva, M. Ritschel, D. Elefant, K. Biedermann, and B. Büchner, Chem. Vap. Deposition **12**, 380 (2006).
[22] A. Winkler, T. Mühl, S. Menzel, R. Kozhuharova-Koseva, S. Hampel, A. Leonhardt, and B. Büchner, J. Appl. Phys. **99**, 104905 (2006).
[23] E. Borowiak-Palen, E. Mendoza, A. Bachmatiuk, M. H. Rummeli, T. Gemming, J. Nogues, V. Skumryev, R. J. Kalenczuk, T. Pichler, and S. R. P. Silva, Chem. Phys. Lett. **421**, 129 (2006).
[24] M. M. Rahman, M. Kisaku, T. Kishi, D. Matsunaka, W. A. Dino, H. Nakanishi, and H. Kasai, J. Phys.: Condens. Matter **16**, S5755 (2004).
[25] Y. J. Kang, J. Choi, C. Y. Moon, and K. J. Chang, Phys. Rev. B **71**, 115441 (2005).
[26] M. Weissmann, G. García, M. Kiwi, R. Ramírez, and C.-C. Fu, Phys. Rev. B **73**, 125435 (2006).
[27] W. Y. Choi, J. W. Kang, and H. J. Hwang, Phys. Rev. B **68**, 193405 (2003).
[28] C. K. Yang, J. Zhao, and J. P. Lu, Phys. Rev. Lett. **90**, 257203 (2003).
[29] E. K. Storms, *Refractory Carbides* (Academic Press, New York, 1968).
[30] H. Chen, R. B. Huang, Z. C. Tang, L. S. Zheng, G. W. Zhou, and Z. Zhang, Appl. Phys. Lett. **77**, 91 (2000).
[31] J. Jiao and S. Seraphin, J. Appl. Phys. **83**, 2442 (1998).
[32] L. E. Toth, *Transition Metal Carbides and Nitrides* (Academic Press, New York, 1971).
[33] D. Porezag, T. Frauenheim, T. Köhler, G. Seifert, and R. Kascher, Phys. Rev. B **51**, 12947 (1995).
[34] M. Elstner, D. Porezag, G. Jungnickel, J. Elsner, M. Haugk, Th. Frauenheim, S. Suhai, and G. Seifert, Phys. Rev. B **58**, 7260 (1998).
[35] C. Köhler, G. Seifert, U. Gerstmann, M. Elstner, H. Overhof, and Th. Frauenheim, Phys. Chem. Chem. Phys. **3**, 5109 (2001).
[36] V. V. Ivanovskaya and G. Seifert, Solid State Commun. **130**, 175 (2004).
[37] V. V. Ivanovskaya, T. Heine, S. Gemming, and G. Seifert, Phys. Status Solidi B **243**, 1757 (2006).
[38] A. Enyaschin, S. Gemming, T. Heine, G. Seifert, and L. Zhechkov, Phys. Chem. Chem. Phys. **8**, 3320 (2006).
[39] J. Häglund, G. Grimvall, and T. Jarlborg, Phys. Rev. B **44**, 2914 (1991).
[40] J. Häglund, G. Grimvall, T. Jarlborg, and A. F. Guillermet, Phys. Rev. B **43**, 14400 (1991).
[41] M. B. Stearns, in *Landolt-Börnstein: Numerical Data and Functional Relationships in Science and Technology*, Vol. 19, edited by H. P. J. Wijn (Springer-Verlag, Berlin, 1986). The DFTB method gives a value for the magnetic moment of bulk bcc iron of $2.0\mu B/\text{atom}$, compared with the experimental values $\sim 2.2\mu B/\text{atom}$.
[42] C. Köhler, G. Seifert, and Th. Frauenheim, Chem. Phys. **309**, 23 (2005).